Azimuthal angle distributions of leptons in the Wigner function approach

Wolfgang Schäfer [1], Mariola Kłusek-Gawenda [1], Antoni Szczurek [1]

[1] Institute of Nuclear Physics, Polish Academy of Sciences, Kraków

UPC 2023: International workshop on the physics of Ultra Peripheral Collisions
December 10-15, 2023, Playa del Carmen, Mexico

Outline

1. Peripheral/ultraperipheral collisions
   - Weizsäcker-Williams equivalent photons
   - a part of the partonic structure of charged particles

2. From ultraperipheral to semicentral collisions
   - dileptons from $\gamma\gamma$ production vs thermal dileptons from plasma phase
   - Wigner function generalization of the Weizsäcker-Williams approach

M. Kłusek-Gawenda, R. Rapp, W. S. and A. Szczurek, "Dilepton Radiation in Heavy-Ion Collisions at Small Transverse Momentum," Phys. Lett. B **790** (2019) 339 [arXiv:1809.07049 [nucl-th]].

M. Kłusek-Gawenda, W. S. and A. Szczurek, "Centrality dependence of dilepton production via $\gamma\gamma$ processes from Wigner distributions of photons in nuclei," Phys. Lett. B **814** (2021), 136114 [arXiv:2012.11973 [hep-ph]].

B. Linek, A. Łuszczak, M. Łuszczak, R. Pasechnik, W. S. and A. Szczurek, "Probing proton structure with $c\bar{c}$ correlations in ultraperipheral pA collisions," JHEP **10** (2023), 179 [arXiv:2308.00457 [hep-ph]].

Dilepton production in semi-central collisions

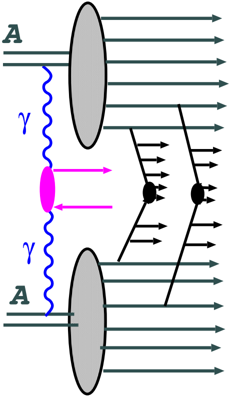

- dileptons from $\gamma\gamma$ fusion have peak at very low pair transverse momentum.
- can they be visible even in semi-central collisions?
- WW photons are a coherent "parton cloud" of nuclei, which can collide and produce particles. Nuclei create an "underlying event, in which e.g. plasma can be formed.
- Early considerations in N. Baron and G. Baur, Z. Phys. C **60** (1993).
- Dileptons are a "classic" probe of the QGP: medium modifications of ρ, thermal dileptons... What is the competition between the different mechanisms?
- dependence on **centrality/ impact parameter**?
- role of photon polarizations

Dilepton production in semi-central collisions

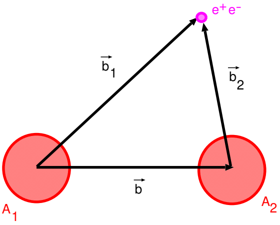

$$\frac{d\sigma_{ll}}{d\xi d^2\boldsymbol{b}} = \int d^2\boldsymbol{b}_1 d^2\boldsymbol{b}_2 \, \delta^{(2)}(\boldsymbol{b} - \boldsymbol{b}_1 - \boldsymbol{b}_2) N(\omega_1, b_1) N(\omega_2, b_2) \frac{d\sigma(\gamma\gamma \to l^+l^-; \hat{s})}{d(-\hat{t})} \ ,$$

where the phase space element is $d\xi = dy_+ dy_- dp_t^2$ with $y_\pm$, p_t and m_l the single-lepton rapidities, transverse momentum and mass, respectively, and

$$\omega_1 = \frac{\sqrt{p_t^2 + m_l^2}}{2} \left(e^{y_+} + e^{y_-}\right) \ , \ \omega_2 = \frac{\sqrt{p_t^2 + m_l^2}}{2} \left(e^{-y_+} + e^{-y_-}\right) \ , \ \hat{s} = 4\omega_1\omega_2 \ .$$

- we adopt the impact parameter definition of centrality

$$\frac{dN_{ll}[\mathcal{C}]}{dM} = \frac{1}{f_{\mathcal{C}} \cdot \sigma^{\rm in}_{\rm AA}} \int_{b_{\rm min}}^{b_{\rm max}} db \int d\xi \, \delta(M - 2\sqrt{\omega_1\omega_2}) \, \frac{d\sigma_{ll}}{d\xi db}\Big|_{\rm cuts} \ ,$$

Thermal dilepton production

- The calculation of thermal dilepton production from a near-equilibrated medium follows the approach of R. Rapp and E. V. Shuryak, Phys. Lett. B **473** (2000); J. Ruppert, C. Gale, T. Renk, P. Lichard and J. I. Kapusta, Phys. Rev. Lett. **100** (2008). R. Rapp and H. van Hees, Phys. Lett. B **753** (2016) 586.
- To compute dilepton invariant-mass spectra an integration of the thermal emission rate over the space-time evolution of the expanding fireball is performed,

$$\frac{dN_{ll}}{dM} = \int d^4x \; \frac{M d^3P}{P_0} \; \frac{dN_{ll}}{d^4x d^4P} \; ,$$

  where $(P_0, \vec{P})$ and $M = \sqrt{P_0^2 - P^2}$ are the 4-vector ($P = |\vec{P}|$) and invariant mass of the lepton pair, respectively.
- The thermal emission rate is expressed through the EM spectral function,

$$\frac{dN_{ll}}{d^4x d^4P} = \frac{\alpha_{\mathrm{EM}}^2 L(M)}{\pi^3 M^2} \; f^B(P_0; T) \; (-g_{\mu\nu}) \mathrm{Im}\Pi_{\mathrm{EM}}^{\mu\nu}(M, P; \mu_B, T) \; ,$$

- The fireball evolves through both QGP and hadronic phases. For the respective spectral functions we employ in-medium quark-antiquark annihilation and in-medium vector spectral functions in the hadronic sector.
- Different centrality classes for different colliding systems are characterized by the measured hadron multiplicities and appropriate initial conditions for the fireball.

Dilepton production in semi-central collisions

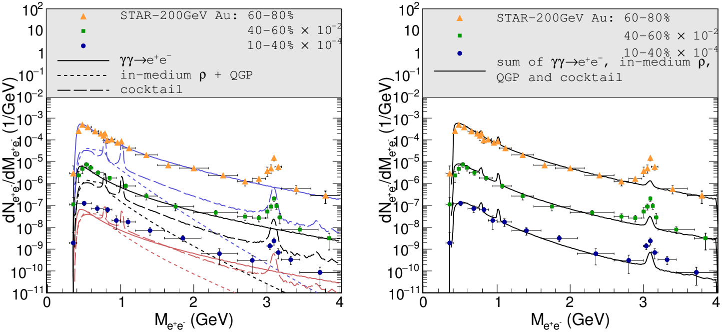

Left panel: Dielectron invariant-mass spectra for pair-P_T<0.15 GeV in Au+Au($\sqrt{s_{NN}}$=200 GeV) collisions for 3 centrality classes including experimental acceptance cuts (p_t >0.2 GeV, $|\eta_e|$<1 and $|y_{e^+e^-}|$<1) for $\gamma\gamma$ fusion (solid lines), thermal radiation (dotted lines) and the hadronic cocktail (dashed lines); right panel: comparison of the total sum (solid lines) to STAR data [1].

[1] data from J. Adam *et al.* [STAR Collaboration], Phys. Rev. Lett. **121** (2018) 132301.

- also added is a contribution from decays of final state hadrons "cocktail" supplied by STAR.
- the J/ψ contribution has been described e.g. in W. Zha, L. Ruan, Z. Tang, Z. Xu and S. Yang, Phys. Lett. B **789** (2019), 238-242 [arXiv:1810.02064 [hep-ph]].

Pair transverse momentum distribution

- Here we perform a simplified calculation by using b-integrated transverse momentum dependent photon fluxes,

$$\frac{dN(\omega, q_t^2)}{d^2\vec{q}_t} = \frac{Z^2\alpha_{EM}}{\pi^2} \frac{q_t^2}{[q_t^2 + \frac{\omega^2}{\gamma^2}]^2} F_{\rm em}^2(q_t^2 + \frac{\omega^2}{\gamma^2}).$$

$$\frac{d\sigma_{ll}}{d^2\vec{P}_T} = \int \frac{d\omega_1}{\omega_1} \frac{d\omega_2}{\omega_2} d^2\vec{q}_{1t} d^2\vec{q}_{2t} \frac{dN(\omega_1, q_{1t}^2)}{d^2\vec{q}_{1t}} \frac{dN(\omega_2, q_{2t}^2)}{d^2\vec{q}_{2t}} \delta^{(2)}(\vec{q}_{1t}+\vec{q}_{2t}-\vec{P}_T)\hat{\sigma}(\gamma\gamma \to l^+l^-)\Big|_{\rm cut}$$

- analogous to TMD-factorization in hard processes. Note that experiment includes a cut $p_t(\text{lepton}) > 0.2\,\text{GeV}$. Formfactors ensure that photon virtualities are much smaller then this "hard scale". We can thus treat them as on-shell in the $\gamma\gamma \to e^+e^-$ cross section.
- notice the extremely sharp peak in q_t, which is cut off only by ω/γ. The peak will move towards smaller q_t as the boost γ increases.
- This approach does not account for **photon polarization** nor **impact parameter dependence**.

Dilepton production in semi-central collisions

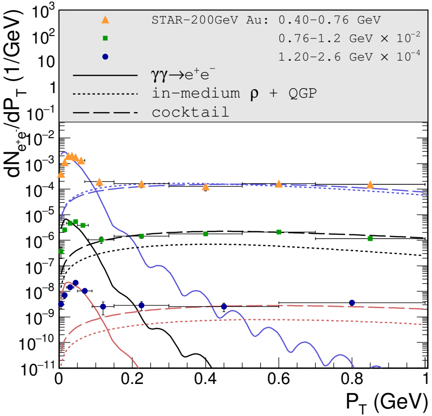

P_T spectra of the individual contributions (line styles as in the previous figure) in 3 different mass bins for 60-80% central Au+Au collisions ($\sqrt{s_{NN}}$=200 GeV), compared to STAR data [1].

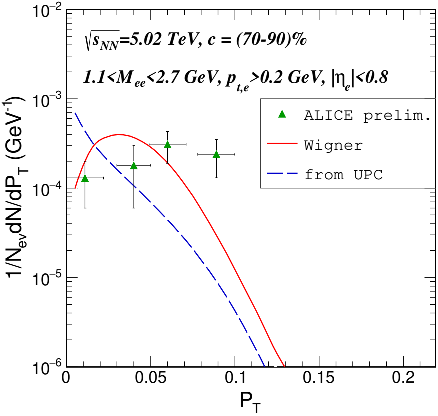

P_T distribution of the pair against ALICE data.

[1] J. Adam *et al.* [STAR Collaboration], Phys. Rev. Lett. **121** (2018) 132301.

Wigner function approach

- We need to find a generalization of photon fluxes (or parton distributions), that contain information on both impact parameter and transverse momentum. This is achieved by the **Wigner function**.
- We also have to take into account photon polarizations, so in fact we obtain a **density matrix** of Wigner functions:

$$N_{ij}(\omega, \boldsymbol{b}, \boldsymbol{q}) = \int \frac{d^2\boldsymbol{Q}}{(2\pi)^2} \exp[-i\boldsymbol{b}\boldsymbol{Q}]\, E_i\Big(\omega, \boldsymbol{q} + \frac{\boldsymbol{Q}}{2}\Big) E_j^*\Big(\omega, \boldsymbol{q} - \frac{\boldsymbol{Q}}{2}\Big)$$

- when summed over polarizations it reduces to the well-known WW flux after integrating over $\boldsymbol{q}$, and to the TMD photon flux after integrating over $\boldsymbol{b}$:

$$\begin{aligned} N(\omega, \boldsymbol{q}) &= \delta_{ij} \int d^2\boldsymbol{b}\, N_{ij}(\omega, \boldsymbol{b}, \boldsymbol{q}) = \delta_{ij}\, E_i(\omega, \boldsymbol{q}) E_j^*(\omega, \boldsymbol{q}) = \Big|\boldsymbol{E}(\omega, \boldsymbol{q})\Big|^2, \\ N(\omega, \boldsymbol{b}) &= \delta_{ij} \int \frac{d^2\boldsymbol{q}}{(2\pi)^2} N_{ij}(\omega, \boldsymbol{b}, \boldsymbol{q}) = \delta_{ij}\, E_i(\omega, \boldsymbol{b}) E_j^*(\omega, \boldsymbol{b}) = \Big|\boldsymbol{E}(\omega, \boldsymbol{b})\Big|^2. \end{aligned}$$

- Field strength vector:

$$\boldsymbol{E}(\omega, \boldsymbol{q}) \propto \frac{\boldsymbol{q} F(q^2)}{\boldsymbol{q}^2 + \frac{\omega^2}{\gamma^2}}$$

Wigner function approach

- The Wigner function is the Fourier transform of a generalized transverse momentum distribution (GTMD), and in some sense (at small-x) the most general function in the zoo of parton correlators. For the photon case, see S. Klein, A. H. Mueller, B. W. Xiao and F. Yuan, Phys. Rev. D **102** (2020) no.9, 094013.
- Recently, there has been a lot of interest in the gluon Wigner distributions, which has applications in exclusive diffractive processes. See e.g. Y. Hagiwara, Y. Hatta, R. Pasechnik, M. Tasevsky and O. Teryaev, Phys. Rev. D **96** (2017) no.3, 034009.
  Review: R. Pasechnik, M Tasevsky (2023)
- In our case we have the simple factorization formula for the cross section:

$$\begin{aligned} \frac{d\sigma}{d^2\boldsymbol{b}d^2\boldsymbol{P}} &= \int d^2\boldsymbol{b}_1 d^2\boldsymbol{b}_2\, \delta^{(2)}(\boldsymbol{b}-\boldsymbol{b}_1+\boldsymbol{b}_2) \int \frac{d\omega_1}{\omega_1}\frac{d\omega_2}{\omega_2} d^2\boldsymbol{q}_1 d^2\boldsymbol{q}_2\, \delta^{(2)}(\boldsymbol{P}-\boldsymbol{q}_1-\boldsymbol{q}_2) \\ &\times \quad N_{ij}(\omega_1,\boldsymbol{b}_1,\boldsymbol{q}_1) N_{kl}(\omega_2,\boldsymbol{b}_2,\boldsymbol{q}_2)\, \frac{1}{2\hat{s}} M_{ik} M^\dagger_{jl}\, d\Phi(l^+l^-). \end{aligned}$$

- no independent sum over photon polarizations!
- other approaches: M. Vidovic, M. Greiner, C. Best and G. Soff, Phys. Rev. **C47** (1993); K. Hencken, G. Baur and D. Trautmann, Phys. Rev. C **69** (2004) 054902; S. Klein et al. (2020).

Wigner function approach

$$
\begin{aligned}
\frac{d\sigma}{d^2\boldsymbol{b}d^2\boldsymbol{P}} &= \int \frac{d^2\boldsymbol{Q}}{(2\pi)^2}\exp[-i\boldsymbol{b}\boldsymbol{Q}]\int \frac{d\omega_1}{\omega_1}\frac{d\omega_2}{\omega_2}\int \frac{d^2\boldsymbol{q}_1}{\pi}\frac{d^2\boldsymbol{q}_2}{\pi}\,\delta^{(2)}(\boldsymbol{P}-\boldsymbol{q}_1-\boldsymbol{q}_2)\\
&\times\; E_i\left(\omega_1,\boldsymbol{q}_1+\frac{\boldsymbol{Q}}{2}\right)E_j^*\left(\omega_1,\boldsymbol{q}_1-\frac{\boldsymbol{Q}}{2}\right)E_k\left(\omega_2,\boldsymbol{q}_2-\frac{\boldsymbol{Q}}{2}\right)E_l^*\left(\omega_2,\boldsymbol{q}_2+\frac{\boldsymbol{Q}}{2}\right)\\
&\times\; \frac{1}{2\hat{s}}\sum_{\lambda\bar{\lambda}} M_{ik}^{\lambda\bar{\lambda}}M_{jl}^{\lambda\bar{\lambda}\dagger}\,d\Phi(l^+l^-).
\end{aligned}
$$

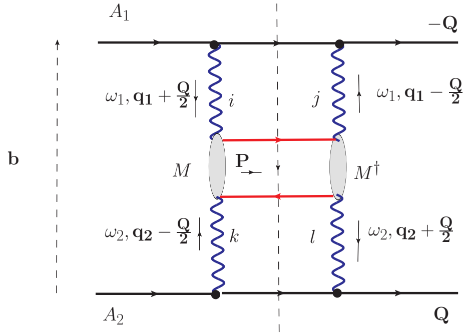

Wigner function approach

$$
\begin{aligned}
\frac{d\sigma}{d^2\boldsymbol{b}d^2\boldsymbol{P}} &= \int \frac{d^2\boldsymbol{Q}}{(2\pi)^2}\exp[-i\boldsymbol{b}\boldsymbol{Q}] \int \frac{d\omega_1}{\omega_1}\frac{d\omega_2}{\omega_2}\int \frac{d^2\boldsymbol{q}_1}{\pi}\frac{d^2\boldsymbol{q}_2}{\pi}\,\delta^{(2)}(\boldsymbol{P}-\boldsymbol{q}_1-\boldsymbol{q}_2) \\
&\times \quad E_i\left(\omega_1,\boldsymbol{q}_1+\frac{\boldsymbol{Q}}{2}\right)E_j^*\left(\omega_1,\boldsymbol{q}_1-\frac{\boldsymbol{Q}}{2}\right)E_k\left(\omega_2,\boldsymbol{q}_2-\frac{\boldsymbol{Q}}{2}\right)E_l^*\left(\omega_2,\boldsymbol{q}_2+\frac{\boldsymbol{Q}}{2}\right) \\
&\times \quad \frac{1}{2\hat{s}}\sum_{\lambda\bar{\lambda}} M_{ik}^{\lambda\bar{\lambda}}M_{jl}^{\lambda\bar{\lambda}\dagger}\,d\Phi(l^+l^-).
\end{aligned}
$$

with

$$
\begin{aligned}
\sum_{\lambda\bar{\lambda}} M_{ik}^{\lambda\bar{\lambda}}M_{jl}^{\lambda\bar{\lambda}\dagger} &= \delta_{ik}\delta_{jl}\sum_{\lambda\bar{\lambda}}\left|M_{\lambda\bar{\lambda}}^{(0,+)}\right|^2 + \epsilon_{ik}\epsilon_{jl}\sum_{\lambda\bar{\lambda}}\left|M_{\lambda\bar{\lambda}}^{(0,-)}\right|^2 \\
&+ \quad P_{ik}^{\parallel}P_{jl}^{\parallel}\sum_{\lambda\bar{\lambda}}\left|M_{\lambda\bar{\lambda}}^{(2,-)}\right|^2 + P_{ik}^{\perp}P_{jl}^{\perp}\sum_{\lambda\bar{\lambda}}\left|M_{\lambda\bar{\lambda}}^{(2,+)}\right|^2 + \text{interferences}
\end{aligned}
$$

$$
\delta_{ik} = \hat{x}_i\hat{x}_k+\hat{y}_i\hat{y}_k,\ \ \epsilon_{ik}=\hat{x}_i\hat{y}_k-\hat{y}_i\hat{x}_k,\ \ P_{ik}^{\parallel}=\hat{x}_i\hat{x}_k-\hat{y}_i\hat{y}_k,\ \ P_{ik}^{\perp}=\hat{x}_i\hat{y}_k+\hat{y}_i\hat{x}_k
$$

- In the $\gamma\gamma$ CM, colliding photons can be in the $J_z=0,\pm 2$ states.

- Wigner function is not necessarily a non-negative function. One may doubt, whether our cross section is manifestly positive, i.e. well-defined. To this end, we can introduce:

$$G_{ik}(\omega_1,\omega_2,\boldsymbol{P};\boldsymbol{b}) \equiv \int \frac{d^2\boldsymbol{k}}{2\pi^2} \exp[-i\boldsymbol{b}\boldsymbol{k}]\, E_i(\omega_1,\boldsymbol{k}) E_k(\omega_2,\boldsymbol{P}-\boldsymbol{k})\,,$$

so that our cross section takes the form

$$\frac{d\sigma}{d^2\boldsymbol{b}d^2\boldsymbol{P}} = \int \frac{d\omega_1}{\omega_1}\frac{d\omega_2}{\omega_2} G_{ik}(\omega_1,\omega_2,\boldsymbol{P};\boldsymbol{b}) G^*_{jl}(\omega_1,\omega_2,\boldsymbol{P};\boldsymbol{b}) \frac{1}{2\hat{s}} \sum_{\lambda\bar\lambda} M^{\lambda\bar\lambda}_{ik} M^{\lambda\bar\lambda\dagger}_{jl}\, d\Phi(l^+l^-)\,.$$

from which we obtain the cross section as a sum of squares which is manifestly positive:

$$\begin{aligned}\frac{d\sigma}{d^2\boldsymbol{b}d^2\boldsymbol{P}} &= \int \frac{d\omega_1}{\omega_1}\frac{d\omega_2}{\omega_2}\Big\{ |G_{xx}+G_{yy}|^2 \sum_{\lambda\bar\lambda}\Big|M^{(0,+)}_{\lambda\bar\lambda}\Big|^2 + |G_{xy}-G_{yx}|^2 \sum_{\lambda\bar\lambda}\Big|M^{(0,-)}_{\lambda\bar\lambda}\Big|^2 \\ &+ |G_{xx}-G_{yy}|^2 \sum_{\lambda\bar\lambda}\Big|M^{(2,+)}_{\lambda\bar\lambda}\Big|^2 + |G_{xy}+G_{yx}|^2 \sum_{\lambda\bar\lambda}\Big|M^{(2,-)}_{\lambda\bar\lambda}\Big|^2 \Big\} \frac{d\Phi(l^+l^-)}{2\hat{s}}\,.\end{aligned}$$

Wigner/GTMD function parametrization

- The Wigner function would be most conveniently decomposed into the $O(2)$ tensors introduced before.
- A popular GTMD parametrization is (e.g. Boer et al. 2018):

$$\begin{aligned} G_{ij}(x, \boldsymbol{q}, \boldsymbol{Q}) &= \delta_{ij} G_1(x, \boldsymbol{q}, \boldsymbol{Q}) + (2q_i q_j - \boldsymbol{q}^2 \delta_{ij}) G_2(x, \boldsymbol{q}, \boldsymbol{Q}) \\ &+ (2Q_i Q_j - \boldsymbol{Q}^2 \delta_{ij}) G_3(x, \boldsymbol{q}, \boldsymbol{Q}) + (q_i Q_j - Q_i q_j) G_4(x, \boldsymbol{q}, \boldsymbol{Q}) \end{aligned}$$

- in the forward limit $\boldsymbol{Q} \to 0$, we have the TMD limits $G_1 \to f_1(x, \boldsymbol{q})$, $G_2 \to h_1^{\perp}(x, \boldsymbol{q})$.
- "Fierz transformation" to convert contractions $P_{ik} P_{jl}$ to $P_{ij} P_{kl}$:

$$\begin{pmatrix} \mathbb{I} \otimes \mathbb{I} \\ \varepsilon \otimes \varepsilon \\ P^{\parallel} \otimes P^{\parallel} \\ P^{\perp} \otimes P^{\perp} \end{pmatrix} \Bigg|_{s-\text{channel}} = \frac{1}{2} \begin{pmatrix} 1 & 1 & 1 & 1 \\ 1 & 1 & -1 & -1 \\ 1 & -1 & 1 & -1 \\ 1 & -1 & -1 & 1 \end{pmatrix} \begin{pmatrix} \mathbb{I} \otimes \mathbb{I} \\ \varepsilon \otimes \varepsilon \\ P^{\parallel} \otimes P^{\parallel} \\ P^{\perp} \otimes P^{\perp} \end{pmatrix} \Bigg|_{t-\text{channel}}$$

- for small-x photons all the GTMDs are proportional to each other.

Photon polarization dependence

- Decompose the $\gamma\gamma \to l^+ l^-$ amplitude into channels of total angular momentum projection $J_z = 0, \pm 2$ and even and odd parity, $z =$ LF momentum fraction of lepton.

$$
\begin{aligned}
M^{(0,+)}_{\uparrow\uparrow} &= \frac{m k_\perp e^{-i\phi}}{k_\perp^2 + m^2}\,, \qquad M^{(0,+)}_{\downarrow\downarrow} = \frac{-m k_\perp e^{i\phi}}{k_\perp^2 + m^2}\,,\\
M^{(0,+)}_{\uparrow\downarrow} &= \frac{m^2(2z-1)}{k_\perp^2 + m^2}\,, \qquad M^{(0,+)}_{\downarrow\uparrow} = \frac{m^2(2z-1)}{k_\perp^2 + m^2}\,,\\
M^{(0,-)}_{\uparrow\uparrow} &= \frac{m k_\perp e^{-i\phi}}{k_\perp^2 + m^2}\,, \qquad M^{(0,-)}_{\downarrow\downarrow} = \frac{m k_\perp e^{i\phi}}{k_\perp^2 + m^2}\,,\\
M^{(0,-)}_{\uparrow\downarrow} &= \frac{-m^2}{k_\perp^2 + m^2}\,, \qquad M^{(0,-)}_{\downarrow\uparrow} = \frac{m^2}{k_\perp^2 + m^2}\,,\\
M^{(2,+)}_{\uparrow\uparrow} &= \frac{-m k_\perp e^{i\phi}}{k_\perp^2 + m^2}\,, \qquad M^{(2,+)}_{\downarrow\downarrow} = \frac{m k_\perp e^{-i\phi}}{k_\perp^2 + m^2}\,,\\
M^{(2,+)}_{\uparrow\downarrow} &= \frac{-k_\perp^2(z e^{i2\phi} - (1-z)e^{-i2\phi})}{k_\perp^2 + m^2}\,, \qquad M^{(2,+)}_{\downarrow\uparrow} = \frac{k_\perp^2((1-z)e^{i2\phi} - z e^{-i2\phi})}{k_\perp^2 + m^2}\,,\\
M^{(2,-)}_{\uparrow\uparrow} &= \frac{m k_\perp e^{i\phi}}{k_\perp^2 + m^2}\,, \qquad M^{(2,-)}_{\downarrow\downarrow} = \frac{m k_\perp e^{-i\phi}}{k_\perp^2 + m^2}\,,\\
M^{(2,-)}_{\uparrow\downarrow} &= \frac{-k_\perp^2(z e^{i2\phi} + (1-z)e^{-i2\phi})}{k_\perp^2 + m^2}\,, \qquad M^{(2,-)}_{\downarrow\uparrow} = \frac{k_\perp^2((1-z)e^{i2\phi} + z e^{-i2\phi})}{k_\perp^2 + m^2}\,,
\end{aligned}
$$

- all amplitudes have a common factor $g_{\rm em}^2/\sqrt{z(1-z)}$.

Polarization structure & angular dependence in the massless case

- for the massless case, only amplitudes for $J_z = \pm 2, S_z = 0$ with $L_z = \pm 2$ contribute!
-

$$\begin{aligned}
\sum_{\lambda\bar{\lambda}} M_{ik}^{\lambda\bar{\lambda}} M_{jl}^{\lambda\bar{\lambda}\dagger} \quad &\Longrightarrow \quad P_{ik}^{\parallel} P_{jl}^{\parallel} \sum_{\lambda=-\bar{\lambda}} \left| M_{\lambda\bar{\lambda}}^{(2,-)} \right|^2 + P_{ik}^{\perp} P_{jl}^{\perp} \sum_{\lambda=-\bar{\lambda}} \left| M_{\lambda\bar{\lambda}}^{(2,+)} \right|^2 \\
&= \quad \frac{2}{k_\perp^2} \left\{ \frac{z^2 + (1-z)^2}{z(1-z)} \left(P_{ik}^{\parallel} P_{jl}^{\parallel} + P_{ik}^{\perp} P_{jl}^{\perp} \right) \right. \\
&+ \quad \left. 2\cos(4\phi) \left(P_{ik}^{\parallel} P_{jl}^{\parallel} - P_{ik}^{\perp} P_{jl}^{\perp} \right) \right\}
\end{aligned}$$

- $\cos(4\phi)$ modulation from **difference between** $\parallel$ **and** $\perp$ **linear** polarizations of "s-channel" photons.
- from Fierz transformation

$$\begin{aligned}
\left(P^{\parallel} \otimes P^{\parallel} + P^{\perp} \otimes P^{\perp} \right)\Big|_{s-\text{channel}} \quad &= \quad \left(\mathbb{I} \otimes \mathbb{I} - \varepsilon \otimes \varepsilon \right)\Big|_{t-\text{channel}} \\
\left(P^{\parallel} \otimes P^{\parallel} - P^{\perp} \otimes P^{\perp} \right)\Big|_{s-\text{channel}} \quad &= \quad \left(P^{\parallel} \otimes P^{\parallel} - P^{\perp} \otimes P^{\perp} \right)\Big|_{t-\text{channel}}
\end{aligned}$$

- In the $\boldsymbol{b}$-integrated cross section, the $\cos(4\phi)$ modulation comes from the **linearly polarized TMD** $h_1^{\perp}(x, q_\perp^2)$ (C. Li, J. Zhou, Y. Zhou (2019)).

Polarization structure & angular dependence, massive case

- In the massive case, relevant to invariant masses close to the threshold, **interferences** between $J_z = 0$ and $J_z = \pm 2$ amplitudes of equal parity can induce the $\cos(2\phi)$ modulation.
- $$\begin{aligned}\sum_{\lambda\bar\lambda} M_{ik}^{\lambda\bar\lambda} M_{jl}^{\lambda\bar\lambda\dagger} \quad \supset \quad & \delta_{ik} P_{jl}^{\parallel} \sum_{\lambda\bar\lambda} M_{\lambda\bar\lambda}^{(0,+)} M_{\lambda\bar\lambda}^{(2,+)\dagger} + P_{ik}^{\parallel} \delta_{jl} \sum_{\lambda\bar\lambda} M_{\lambda\bar\lambda}^{(2,+)} M_{\lambda\bar\lambda}^{(0,+)\dagger} \\ + \quad & \epsilon_{ik} P_{jl}^{\perp} \sum_{\lambda\bar\lambda} M_{\lambda\bar\lambda}^{(0,-)} M_{\lambda\bar\lambda}^{(2,-)\dagger} + P_{ik}^{\perp} \epsilon_{jl} \sum_{\lambda\bar\lambda} M_{\lambda\bar\lambda}^{(2,-)} M_{\lambda\bar\lambda}^{(0,-)\dagger}\end{aligned}$$
- We can expect a different dependence on centrality of the $\cos(2\phi)$ and $\cos(4\phi)$ contributions.
- In the t-channel coupling, the $\boldsymbol{b}$–integrated cross section will contain the product of unpolarized & lineraly polarized TMD's: $f_1(x_1, q_{1\perp}^2) h_1^{\perp}(x_2, q_{2\perp}^2) + (x_1, q_{1\perp} \leftrightarrow x_2, q_{2\perp})$.
- In **diffractive photoproduction of** $q\bar q$ **pairs** $\cos(2n\phi)$ correlations are induced by "elliptic" gluon GTMD/Wigner function(and higher harmonics). The dominant correlation here is $\cos(2\phi)$.

Dilepton production in semi-central collisions

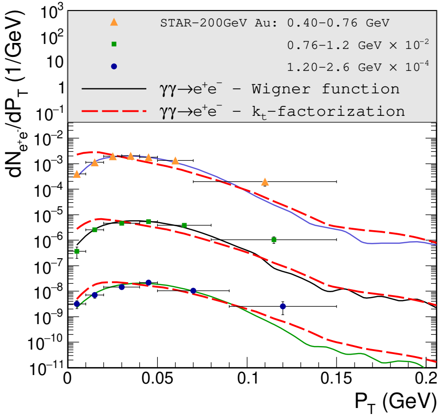

P_T spectra for 60-80% central Au+Au collisions ($\sqrt{s_{\mathrm{NN}}}$=200 GeV).

- Improved description of RHIC data in Wigner-function approach.

Acoplanarity distributions at LHC energies ($\sqrt{s_{NN}} = 5$ TeV)

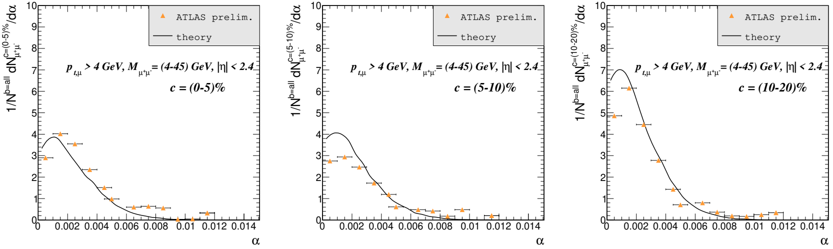

Data from ATLAS, ATLAS-CONF-2019-051

- acoplanarity distribution of dimuons $\alpha = 1 - \frac{\Delta\phi}{\pi}$ in different bins of centrality

Acoplanarity distributions at LHC energies ($\sqrt{s_{NN}} = 5$ TeV)

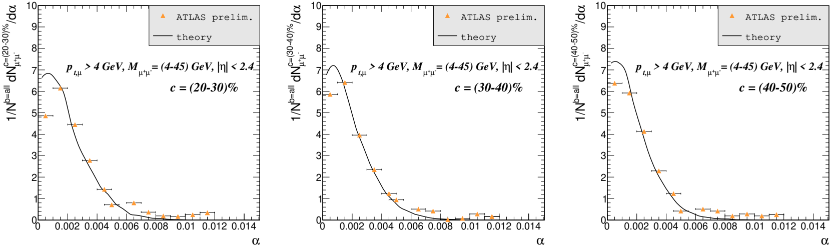

Data from ATLAS, ATLAS-CONF-2019-051

- acoplanarity distribution of dimuons $\alpha = 1 - \frac{\Delta\phi}{\pi}$ in different bins of centrality

Acoplanarity distributions at LHC energies ($\sqrt{s_{NN}} = 5$ TeV)

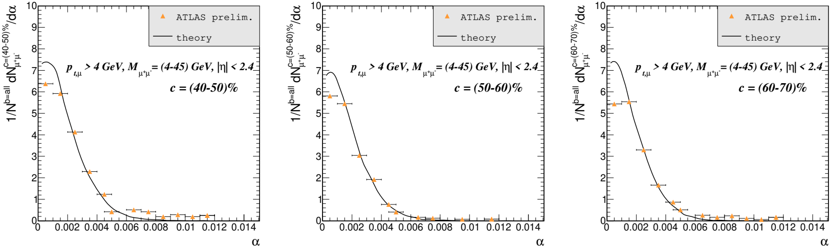

Data from ATLAS, ATLAS-CONF-2019-051

- acoplanarity distribution of dimuons $\alpha = 1 - \frac{\Delta\phi}{\pi}$ in different bins of centrality
- possible corrections: 1. photon emission/Sudakov resummation, genuine **strong field effects**:multiphoton exchanges are enhanced $\propto (Z\alpha)^{n_1+n_2}$, but suppressed for small-size electric dipoles.

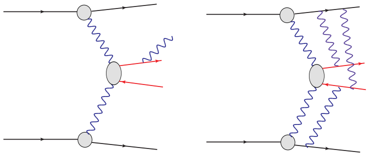

Azimuthal angle distribution

- azimuthal angle between **sum and difference** of lepton transverse momenta.

$$\cos\phi = \frac{\boldsymbol{P}\cdot(\boldsymbol{p}_- - \boldsymbol{p}_+)}{|\boldsymbol{P}||\boldsymbol{p}_- - \boldsymbol{p}_+|} \approx \frac{\boldsymbol{P}\cdot\boldsymbol{k}}{|\boldsymbol{P}||\boldsymbol{k}|}, \qquad \boldsymbol{k} = z_+\boldsymbol{p}_- - z_-\boldsymbol{p}_+ \,.$$

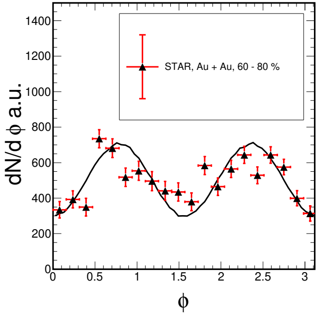

Data from STAR, Phys. Rev. Lett. 127 (2021); experimental cuts: $0.45 < M < 0.76$ GeV, $P_T < 0.1$ GeV.

- $\cos 4\phi$ modulation reflects orbital angular momentum $L_z = 2$ of e^+e^- pair.
- Calculation from Wigner function approach, M. Kłusek-Gawenda, W.S., A. Szczurek, in preparation.

Centrality dependence

- Angular distribution decomposed in harmonics:

$$\frac{dN}{d\phi} \propto 1 + A_2 \cos 2\phi + A_4 \cos 4\phi + \dots$$

$\sqrt{s_{NN}} = 200\,\text{GeV}$	Wigner	Wigner	STAR	STAR
centrality	A_4	$\sqrt{\langle P_T^2 \rangle}$ MeV	A_4	$\sqrt{\langle P_T^2 \rangle}$ MeV
60-80 %	-0.39	47.7	0.27 ± 6	50.9 ± 2.5
40-60 %	-0.49	51.0	—	—
20-40 %	-0.62	54.8	-	-
0-20%	-0.77	59.6	-	-

Table: Centrality dependence of angular coefficient and mean P_T of e^+e^--pair.

Diffractive production of $c\bar{c}$ pairs in pA UPC

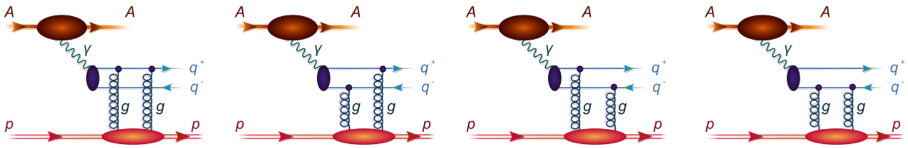

Figure: Feynman diagrams for the diffractive photoproduction of $q\bar{q}$ pairs in nucleus-proton collisions, discussed in the present paper.

$$\frac{d\sigma(\gamma p \to Q\bar{Q}p; s_{\gamma p})}{dz d^2\vec{P}_\perp d^2\vec{\Delta}_\perp} = \overline{\sum_{\lambda_\gamma,\lambda,\bar{\lambda}}} \Big| \int \frac{d^2\vec{b}_\perp d^2\vec{r}_\perp}{(2\pi)^2} e^{-i\vec{\Delta}_\perp\cdot\vec{b}_\perp} e^{-i\vec{P}_\perp\cdot\vec{r}_\perp} N(Y,\vec{r}_\perp,\vec{b}_\perp)\, \Psi^{\lambda_\gamma}_{\lambda\bar{\lambda}}(z,\vec{r}_\perp) \Big|^2 .$$

- Jet momentum $\vec{P}_\perp$, pair transverse momentum $\vec{\Delta}_\perp$.
- Dipole amplitude ⇔ GTMD; dependence on $\cos\phi = \vec{P}_\perp \cdot \vec{\Delta}_\perp/(P_\perp \Delta_\perp$ induced by **elliptic gluon TMD**.

$$\begin{aligned} N(Y,\vec{r}_\perp,\vec{b}_\perp) &= \int d^2\vec{q}_\perp d^2\vec{\kappa}_\perp\, f\left(Y, \frac{\vec{q}_\perp}{2}+\vec{\kappa}_\perp, \frac{\vec{q}_\perp}{2}-\vec{\kappa}_\perp\right) \exp[i\vec{q}_\perp\cdot\vec{b}_\perp] \\ &\times \left\{ \exp\left[i\frac{1}{2}\vec{q}_\perp\cdot\vec{r}_\perp\right] + \exp\left[-i\frac{1}{2}\vec{q}_\perp\cdot\vec{r}_\perp\right] - \exp[i\vec{\kappa}_\perp\cdot\vec{r}_\perp] - \exp[-i\vec{\kappa}_\perp\cdot\vec{r}_\perp] \right\} . \end{aligned}$$

- $$f\left(Y, \frac{\vec{q}_\perp}{2}+\vec{\kappa}_\perp, \frac{\vec{q}_\perp}{2}-\vec{\kappa}_\perp\right) = f_0(Y,\kappa_\perp,q_\perp) + 2\cos(2\phi_{q\kappa})\, f_2(Y,\kappa_\perp,q_\perp) .$$

Diffractive production of $c\bar{c}$ pairs in pA UPC

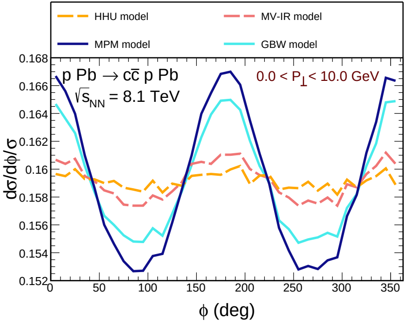

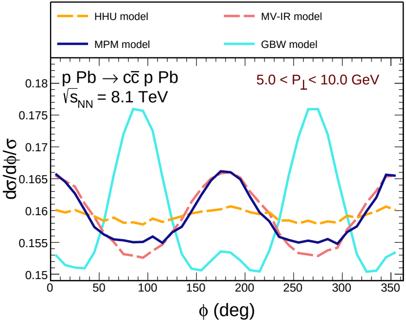

Figure: Distributions in the azimuthal angle ϕ between $\vec{P}_\perp$ and $\vec{\Delta}_\perp$ normalised to the total cross section for $0.01 < P_\perp < 10.0\,\mathrm{GeV}$ on the left and for $5.0 < P_\perp < 10.0\,\mathrm{GeV}$ on the right.

- calculations from B.Linek et al. JHEP **10** (2023), 179.
- in impact parameter space: angular modulation due to dependence on relative orientation of $\vec{b}_\perp$ and $\vec{r}_\perp$!. Can have dynamical origin, as well as a simple geometric one.

Summary

- We have studied low-P_T dilepton production in ultrarelativistic heavy-ion collisions, by a systematic comparisons of thermal radiation and photon-photon fusion within the coherent fields of the incoming nuclei.
- Comparison to recent STAR data: good description of low-P_T dilepton data in Au-Au($\sqrt{s_{NN}}$=200 GeV) collisions in three centrality classes, for invariant masses from threshold to $\sim$4 GeV.
- Coherent emission dominant for the two peripheral samples, and comparable to the cocktail and thermal radiation yields in semi-central collisions.
- Impact-parameter dependent dilepton P_T distribution is described by a Wigner function density matrix generalization of the Weizsäcker-Williams fluxes. Different weights of $J_z = 0, \pm 2$ channels of the $\gamma\gamma$-system. For e^+e^- pairs the $J_z = \pm 2$ channels dominate.
- We obtain an improved description of RHIC data.
- Proper account for the b-dependence is crucial at LHC energies.
- We obtain a very good description of ATLAS azimuthal decorrelations, our predictions agree well with recent ALICE data.
- the azimuthal $\cos 4\phi$ correlation measured by STAR is well reproduced, and can be traced to **orbital angular momentum of leptons**. Photon polarizations play an important role.
- Angular coefficient rises for more central collisions.
- in diffractive heavy quark production, the parton-level $\cos 2\phi$ azimuthal correlations induced by the elliptic Wigner function are much smaller than the ones in the QED process.